International Journal of Aviation Science and Technology

Research Article

Architecture of Stratosphere Rocket for Cubesats

Alper Şanlı[1]*, Tuncay Yunus Erkeç[2], Melih Beceren[3], Mehmet Furkan Kemallı[4]

[1] National Defence University, Institute of Atatürk Strategic Studies and Graduate, Istanbul, Turkey
alpersanli16@gmail.com - 0000-0002-4338-7685

[2] National Defence University, Institute of Atatürk Strategic Studies and Graduate, Istanbul, Turkey
tuncayyunus@gmail.com - 0000-0003-3357-0985

[3] National Defence University, Institute of Atatürk Strategic Studies and Graduate, Istanbul, Turkey
melihbeceren@gmail.com - 0000-0002-8728-0812

[4] Trendyol Group, System Engineer, Ankara, Turkey
kemallifurkan@gmail.com - 0000-0003-2052-3397

Abstract

Cubesat missions are evolving, and because of their high efficiency, they are becoming more common. Cubesats can go to space more easily because of their compact size. Launch vehicles provide great opportunity for us to reach space and high altitudes of the atmosphere. Today, cubesats are launched to high altitudes for experimental purposes with the help of launch vehicles. In this investigation, a novel launch vehicle was created to match the cubesat's specifications. A stable launch vehicle that can take a cubesat the size of 3U to the stratospheric layer has undergone its first design and examination. Flight simulations were carried out by researching the design stages considered in the launch vehicle. The first design of the launch vehicle suitable for the desired task was made and the altitude, stability and drag analyzes that this design could reach were carried out. The design stages and analysis results of the launch vehicle that will deliver the cubesat to the stratosphere layer are shared. In this study, a design exercise for a stratospheric rocket is proposed. Future research will examine the launch vehicle that will cross the space boundary, known as the Kármán line.

Keywords

Launch vehicle
Rocket
Cubestrat
Design
Analysis
Stratosphere

Time Scale of Article

Received 23 August 2022
Revised until 19 May 2023
Accepted 19 May 2023
Online date 28 June 2023

1. Introduction

Since ancient times, people have looked for means to travel to space. With new launch vehicles, it is now simpler to approach the space frontier, or the Kármán line. Cubesats are trained in the stratospheric layer. Every year, more man-made satellites are launched into orbit.

Since cubesat technology has advanced, they have begun to take the role of large satellites. The launch systems' main function is to raise the payload to the required, healthy altitudes. There are low-altitude, medium-altitude, and high-altitude launch methods available based on altitude. In practice, the most used methods to raise the payload to the desired altitude are rocket and atmospheric balloon technologies, which are much more cost-effective (Hall et al., 2020). Rocket propulsion is a class of jet propulsion in which stored mass, known as propellant, is combusted and ejected from the vehicle at high velocity (Balmogim et al., 2015). The launch vehicle is rocket type. Three components make up most launch systems. They are the propulsion subsystem, the structural subsystem, and the payload. A large part of

*: Corresponding Author Alper Şanlı, alpersanli16@gmail.com
DOI: 10.23890/IJAST.vm04is01.0102

launch systems is the propulsion system. There are main classes of propulsion systems; liquid rocket engines, solid rocket engines, hybrid rocket engines, nuclear rocket engines, electric rocket engines (Sutton and Biblarz, 2016). Liquid propellant rocket engines contain complex systems (McCormick et al., 2005). Hybrid rocket technology uses both liquid and solid fuel rockets (Dyer et al., 2007). The use of hybrid rockets is more efficient for launch vehicles (Leverone, 2013). Cesaroni reloadable rocket engines are considered in this study. This technology is convenient and less complex systems (Mahjub et al., 2020). The structural subsystem holds the other subsystems together, ensuring the launch vehicle's in flight integrity. The payload may be experimental, depending on the launch vehicle's mission. Launch vehicles can be employed for scientific, military, and academic endeavors.

Lift and drag on the launch vehicle can only be applied if the launch vehicle is in an atmosphere. The atmosphere consists of troposphere, stratosphere, mesosphere, thermosphere and exosphere layers. The mission of the launch vehicle designed and analyzed in this study is to deliver the cubesat to the stratosphere layer. The stratosphere layer is located between 12 and 50 km. Launching the launch vehicle in different seasons causes approximately 5% change in vehicle performance. The pressure in the stratosphere layer is between 200 mbar and 0 mbar. Atmospheric density is between about 0.3 kg/m^3 and 0 kg/m^3. Temperature values are between -60 °C and 0 °C. The wind speed at this altitude is 10 m/s and 60 m/s.

The launch vehicle that will take the cubesats to the stratospheric layer has been designed and analyzed for this project. Vehicle studies will be conducted in the following stages to transport the cubesats to the Kármán line. A launch vehicle that would send cubesats to the stratospheric layer for educational reasons was investigated before the Kármán line.

2. Overview of Mission

A launch system is created in this study to lift a cubesat intended for educational purposes into the stratospheric layer. Scientific data, image and telemetry data obtained from the atmosphere will be transmitted to the ground station through the sensors on the cube satellite used for educational purposes. There are two stages in the launch system. Three rocket engines are in the first stage, one rocket engine is in the second stage. The cubesat will be positioned in a location on the second level. POD with space for three 3U cubesats. At apogee altitude, POD will assist in releasing the cubesat from the launch vehicle. The sample cubesat model that can be launched with the launch vehicle and the model that can be mounted inside the launch vehicle of the sample cubesat model are shown in Figure 1.

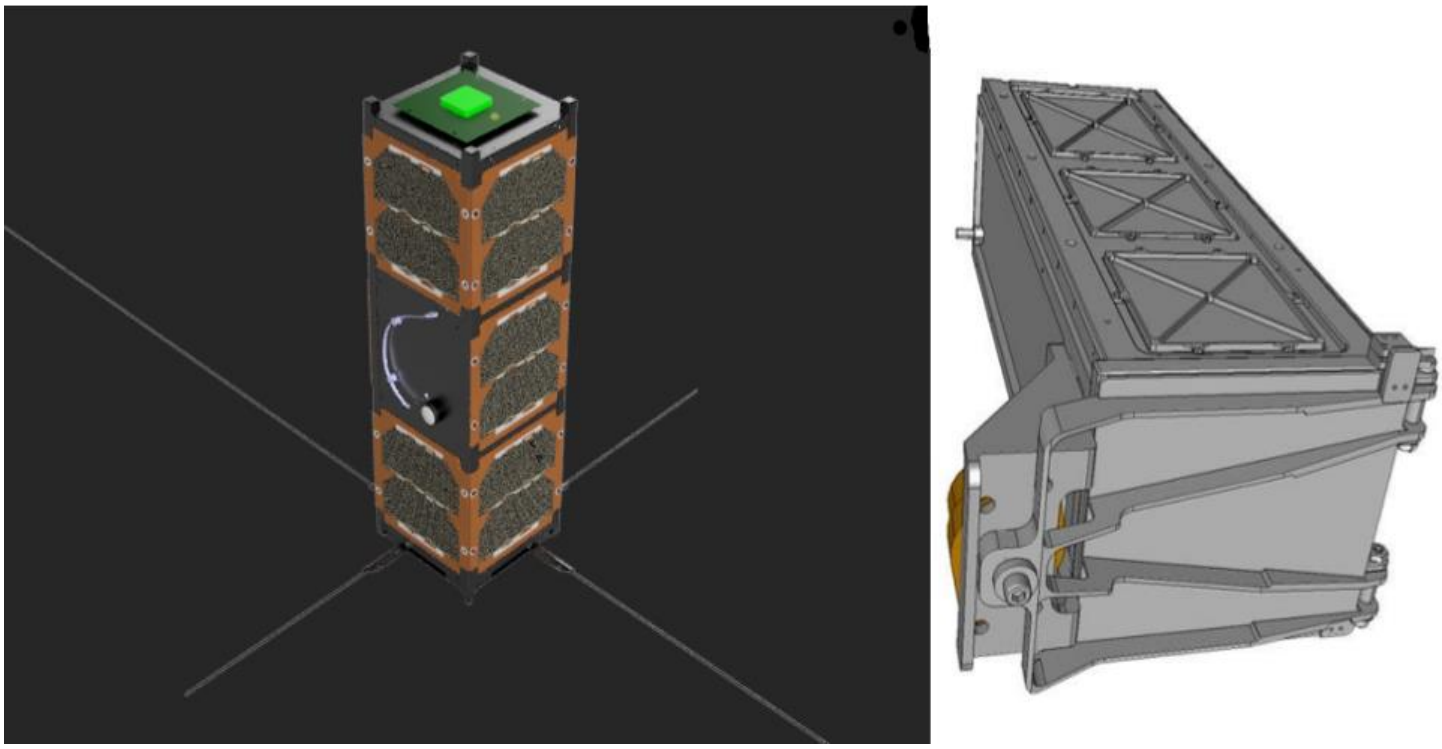

(a) (b)

Fig. 1. (a) Sample cubesat model and exploded view to be placed within the launch vehicle and simulation and (b) example of a cubesat that can be mounted on a launch vehicle (Şanlı and Aslan, 2021) (Johnstone, 2020).

3. Launch Vehicle Architecture and Details

Cubesat launch vehicles are still being developed today. Their goal is to place cubesat on the Kármán line. The launch vehicle must have the boundary conditions to carry the cube satellite. Cubesat dimensions are in 3U standards for this launch vehicle. The created design should be suitable for atmospheric conditions and should not damage the cubesat.

It is possible to classify rockets according to the Mach number. This number is the ratio of the velocity of a moving mass to the speed of sound under the conditions in which the mass is present. There are 6 regimens according to the Mach number. These are subsonic, transonic, supersonic, hypersonic, high-hypersonic and re-entry speeds. The values of Mach regimes are shown in the Table 1.

Table 1. Flight speed values according to regime types

Regime	**Flight Speed**				
	(Mach)	(knots)	(mph)	(km/h)	(m/s)
Subsonic	<0.8	<530	<609	<980	<273
Transonic	0.8-1.2	530-794	609-914	980-1,235	273-409
Supersonic	1.2-5.0	794-3,806	915-3,806	1,235-6,126	410-1,702
Hypersonic	5.0-10.0	3,308-6,615	3,806-7,680	6,126-12,251	1,702-3,403
High-Hypersonic	10.0-25.0	6,615-16,537	7,680-19,031	12,251-30,626	3,403-8508
Re-entry speeds	>25.0	>16,537	19,031	>30,626	8,508

It is a launch vehicle design that reaches supersonic velocity. Vehicles reaching supersonic velocities are in the 1.2–5.0 mach range. Equation 1 contains the formula for Mach number.

$$M=u/c \quad (1)$$

M :Mach number

u :The local flow velocity relative to the limits (m/s)

c :Constant for speed of sound in the medium (m/s)

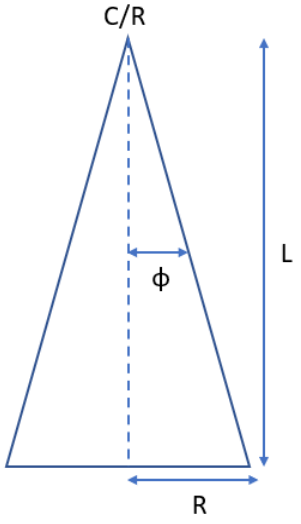

Fig. 2. Nose cone geometry

The maximum velocity of the designed launch vehicle is Mach 3.61. The designed launch vehicle is 419 cm long and weighs roughly 106602 g in total, including the payload. Fiberglass, carbon fiber, aluminum and a composite materials are frequently used materials in the launch vehicle. The strength of the materials is high and it provides structural strength. They are resistant to high temperatures and are lightweight materials. Fiberglass makes up the nose cone, while carbon fiber is used to build the stages and fins.

The boundary conditions of the cubesat must be compatible with the POD dimensions. The cubesat will be placed in a POD portion that is 30 cm long and 17 cm in diameter. On the launch vehicle, the POD section is in the second stage. When the launch vehicle reaches the desired altitude, it will release the cubesat from the POD section with a spring-loaded release mechanism. In this way, the cubesat and the launch vehicle will be separated

Launch systems can use conical, biconical, power series, ogive series, elliptical, parabolic, and haack series nose cones. The coefficient of friction is directly influenced by the nose cone design. The nose cone of the cubesat launch vehicle is conical in shape. Figure 2 shows the geometric design of the conical shape.

The drag coefficient change depending on the nose cone geometry is shown in Figure 3. These are rectangular, wedge, airfoil, rounded geometries. As the nose cone angle increases, the drag coefficient increases.

The variables in Equations 2 and 3 were used to design the nose cone geometry.

$$y = x\frac{R}{L} \quad (2)$$

$$\varphi = tan^{-1}(\frac{R}{L}) \quad (3)$$

x :position in reference plane

y :Position in reference plane

R :The radius of the nose cone

L :The length of the nose cone

φ :nose cone angle)

The nose cone in question weighs 585 g. The length of the nose cone is 600 mm, and the semi-structure is 170 mm. The design values of the nose cone are important for stable flight. Since it is the part that first encounters the fluid air, the drag coefficient should be low.

The dimension and visualization of the launch vehicle are shown in Figure 4. Drag is further reduced by limiting fuselage diameter (using the transonic area rule) at the fin-can section. The vehicle also features a conical tail piece to reduce base drag effects during subsonic flight (Brooks et al., 2010). There are four types of drag acting on the launch vehicle. These are friction drag, pressure drag, induced drag and interference drag (Box et al., 2009). Pressure drag is divided into two. These are wave drag and base drag. Friction drag occurs between the produced material and the fluid. Pressure drag is the difference in force caused by the pressure distribution around the launch vehicle. Wave drag is caused by the force differences that occur during shock waves. Due to the design of the launch vehicle, the velocity of the flow varies, which creates base drag. Induced drag occurs depending on the angle of the launch vehicle. Interference drag is caused by the interaction of the launch vehicle's fuselage and fins. Drag values are important for the launch vehicle to reach the desired altitude steadily.

The launch vehicle has fins that ensure stable flight. There are a total of six ailerons on the first stage and second stage. The blade sections are usually four. These are rounded, airfoil, wedge, rectangular geometries. The rounded blade geometry is easy to manufacture and provides average performance. Airfoil fin geometry is good for subsonic flight. The wedge blade geometry is good for supersonic flight. The rectangular blade geometry is easy to manufacture and has a high drag value. The launch vehicle has a wedge type fin geometry. The types of fins used in the launch vehicle are shown in the Figure 5.

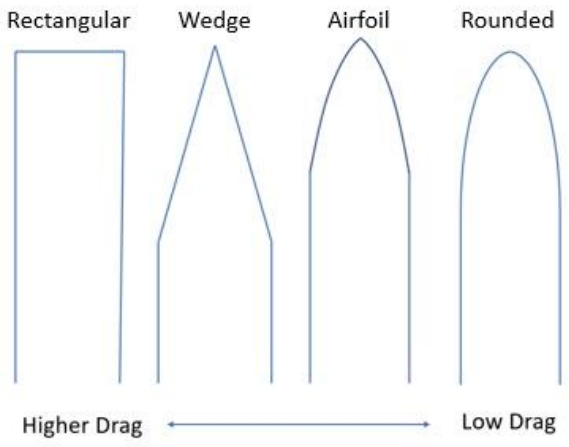

Fig. 3. Drag values according to geometric designs

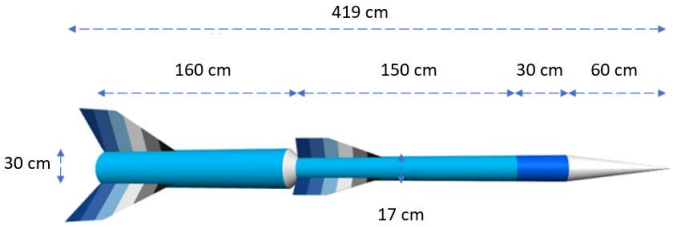

Fig. 4. Image and dimensions of the launch vehicle

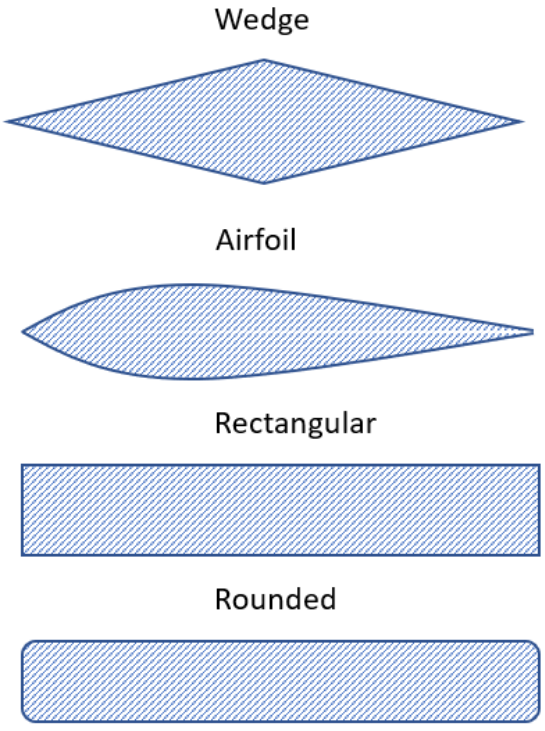

Fig. 5. Launch vehicle fin types.

The conical nose cone's overall drag coefficient was calculated to be 0.02. The center of pressure of the launch vehicle is directly impacted by the fin type chosen. Fins stabilize the launch vehicle because it lacks active control mechanisms. Control mechanisms provide a stabilized flight (Bossert et al., 2003). The

launch vehicle's center of gravity is positioned behind the center of pressure to ensure a steady flight. In total, 6 blades—3 in the first stage and 3 in the second—were employed. Ailerons used in the second stage have a total drag coefficient of 0.02 and blades used in the first stage have a drag value of 0.05. Equation 4 contains the formula for the drag force (Taylor, 2017).

$$F_D = C_d \rho V^2 \frac{A}{2} \quad (4)$$

F_D :Drag force (N)

C_d :Drag coefficient

ρ :Atmospheric density (kg/m^3)

V :Velocity (m/s)

A :Surface area (m^2)

The launch vehicle's architecture is depicted in Figure 6 and consists of two stages connected in series.

The launch vehicle is equipped with reloadable rocket engines. A rocket engine with a cylinder diameter of 161 mm and a length of 597 mm and a total impulse value of 41125 seconds is located in the second stage. Three Cesaroni rocket engines with a combined impulse value of 21041 seconds, a radius of 98 mm, and a length of 1239 mm are located in the first stage. I_s, the equation for the total impulse, is part of Equation 5 (Mishra et al., 2021).

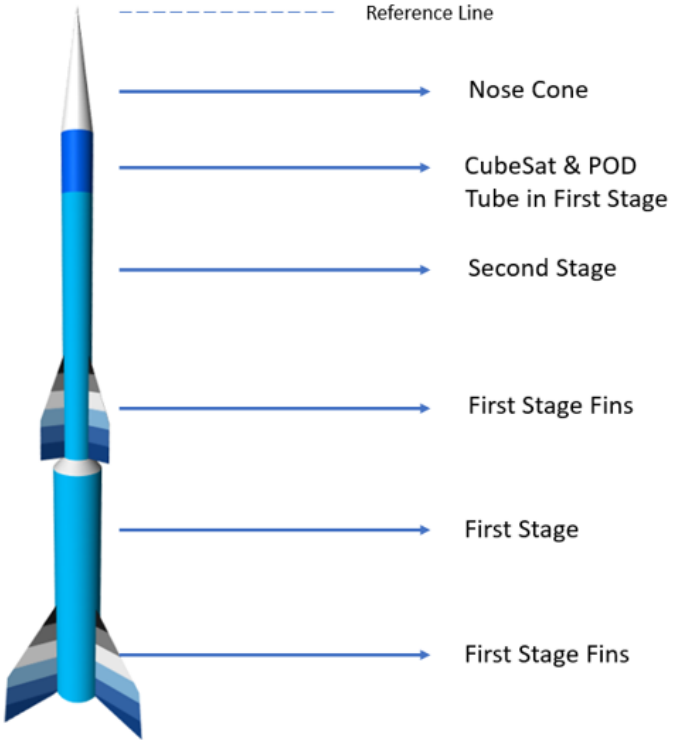

Fig. 6. Design and subsystems for launch vehicle

$$I_s = \frac{\int_0^t F dt}{g_0 \int_0^t \dot{m} dt} \quad (5)$$

$$c = I_s g_0 = \frac{F}{\dot{m}} \quad (6)$$

I_s :The total impulse (s)

F :Force (N)

t :Time (s)

$\dot{m}$:Total fuel mass burn rate (kg/s)

g_0 :Gravity acceleration (m/s^2)

With the help of engine blocks and gripping components, rocket engines are fastened to stage structures. The launch vehicle has a maximum speed of 3.61 Mach, a maximum acceleration of 170 m/s^2, and an apogee of 32676 meters. The launch vehicle's pressure center is 321 cm from the reference plane, whereas the center of gravity is 269 cm from the same reference point.

The center of gravity and center of pressure equations are found in Equation 7 and Equation 8. W (N) stands for the overall weight, c_g (mm) is the distance from the center of gravity to the reference plane, d_n (mm) is the distance of the subsystems from the reference plane, and w_n (N) is the weight of the subsystems. A_n (mm^2) is the surface area of the subsystems, and c_p (mm) is the separation between the center of gravity and the reference plane. The center of gravity and center of pressure on the launch vehicle are shown in Figure 7 and Figure 8.

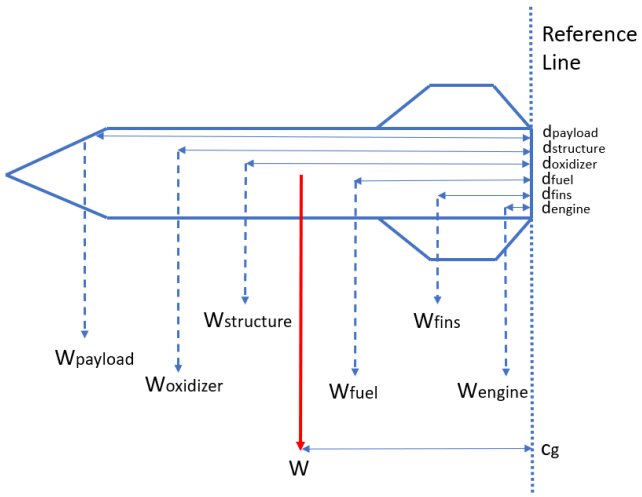

Fig. 7. Center of gravity on the launch vehicle

$$c_g = \frac{w_{payload} d_{payload} + w_{oxidizer} d_{oxidizer} + w_{fuel} d_{fuel} + w_{structure} d_{structure} + w_{engine} d_{engine} + w_{fins} d_{fins}}{W} \quad (7)$$

$$c_p = \frac{a_{payload} d_{payload} + a_{structure} d_{structure} + a_{fins} d_{fins}}{A} \quad (8)$$

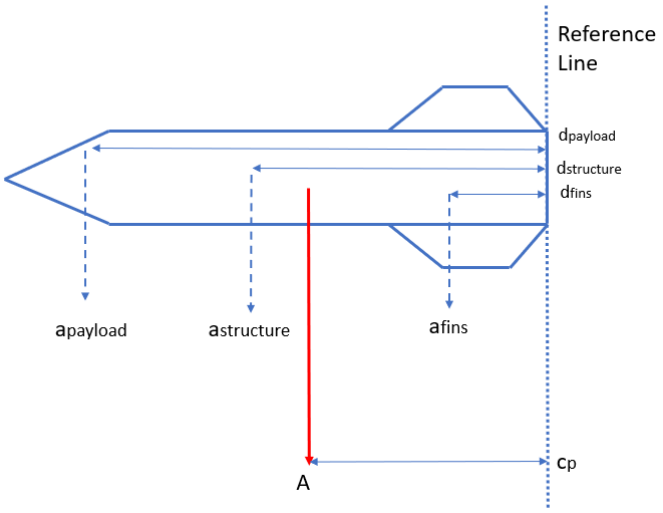

Fig. 8. Center of pressure on the launch vehicle

4. Results of Launch Vehicle Flight Analysis

The altitude, stability, center of pressure, center of gravity, and drag that the launch vehicle will reach during its flight are analyzed. The launch vehicle's stability is directly impacted by the position of the center of gravity and the center of pressure. It can ascend vertically due to its stability.

The launch vehicle consists of two stages. When the altitude of 2 km is reached, the first stage of the launch vehicle leaves. The first stage leaves the launch vehicle after 10-12 seconds. The second stage of the launch vehicle reaches an altitude of about 32 km and releases the cube satellite at the highest altitude. The launch vehicle reaches the highest altitude during 78-82 seconds of flight.

The total flight time of the launch vehicle took 725 seconds. The launch vehicle's total altitude values are shown in Figure 9.

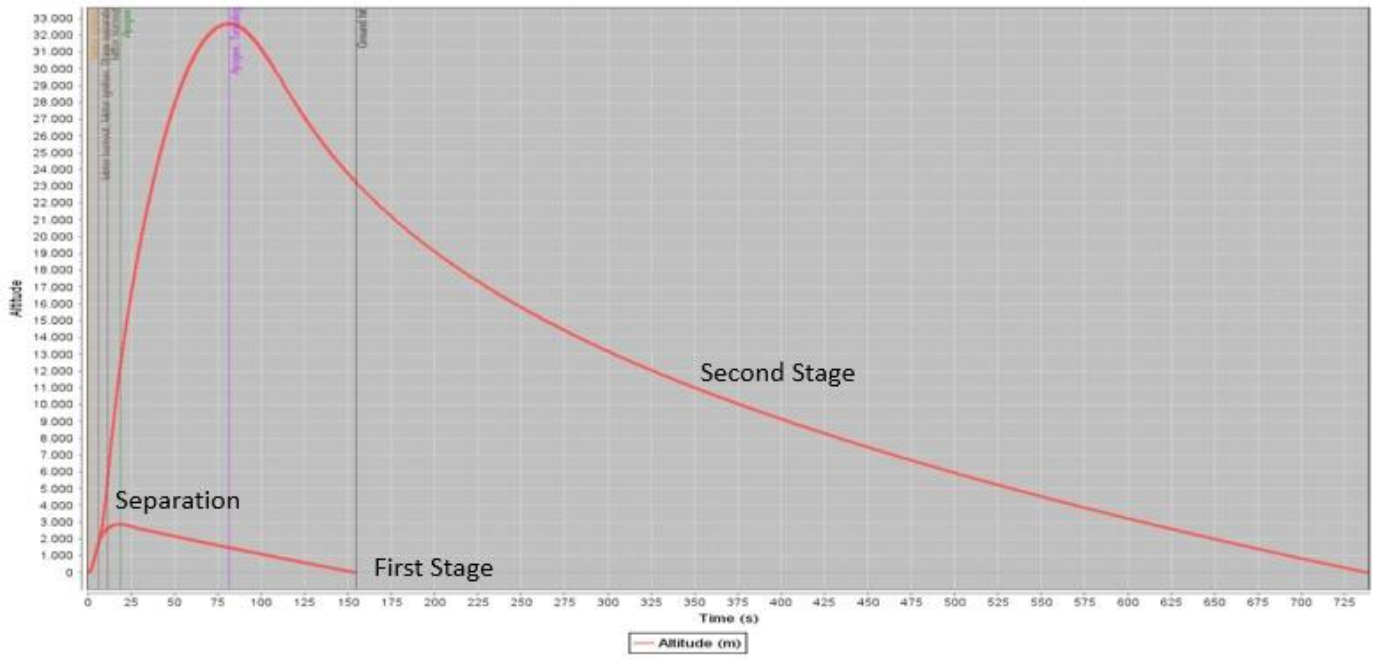

Fig. 9. Total altitude of the launch vehicle graph

The first stage of the launch vehicle split at about 3000 meters. This separation is shown by the red line in Figure 9. The second stage of the rocket reached an altitude of 32676 m. This is shown with a red line in Figure 10. The stable flight of the launch vehicle depends on the center of gravity and the center of pressure. During the flight, the center of gravity must be in front of the center of pressure in the reference plane so that the launch rocket can reach the highest altitude. The parachute will prevent the launch vehicle from being damaged by reducing its speed during its fall (Chowdhury, 2012). Parachute rescue will be made for the launch vehicle.

During the first 10 seconds of flight, the center of pressure is on average 100 cm behind the center of gravity. With the realization of the stage separation, the center of gravity is on average 25 cm ahead of the pressure center during the 80 seconds when the highest altitude is reached.

The shifts in the launch vehicle's center of gravity and center of pressure are depicted in Figure 10 over the course of its entire flight. The flight demonstrated a steady flying because the center of pressure did not cross in front of the center of gravity. It was discovered that the stability value was always positive.

In Figure 10, the Cp value changed from 320 mm to 150 mm at 8 seconds; Cg value decreased from 250 mm to

150 mm. This is because the first stage is separated from the launch vehicle. Throughout the duration of flight, the launch vehicle is subject to drag, which has an impact on its stability and altitude. The launch vehicle is exposed to friction drag, pressure drag, induced drag and interference drag during flight. The resulting shock wave is effective in the structure of the launch vehicle and in the formation of atmospheric drag. The pressure differences that occur in the launch vehicle structure during the flight cause different forces to act on each area of the launch vehicle.

According to the mach number value, the values of the drag coefficient, friction drag coefficient, base drag coefficient, and pressure drag coefficient are shown in Figure 11.

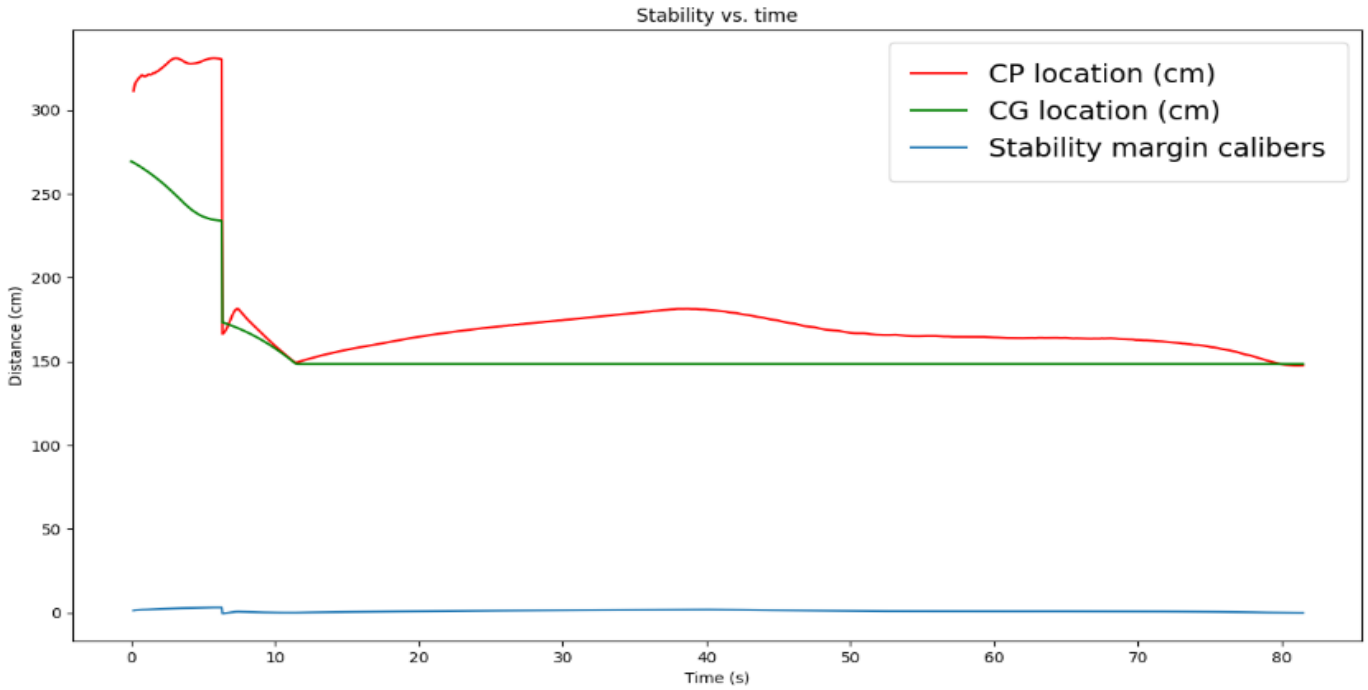

Fig. 10. Graph of launch vehicle stability over time

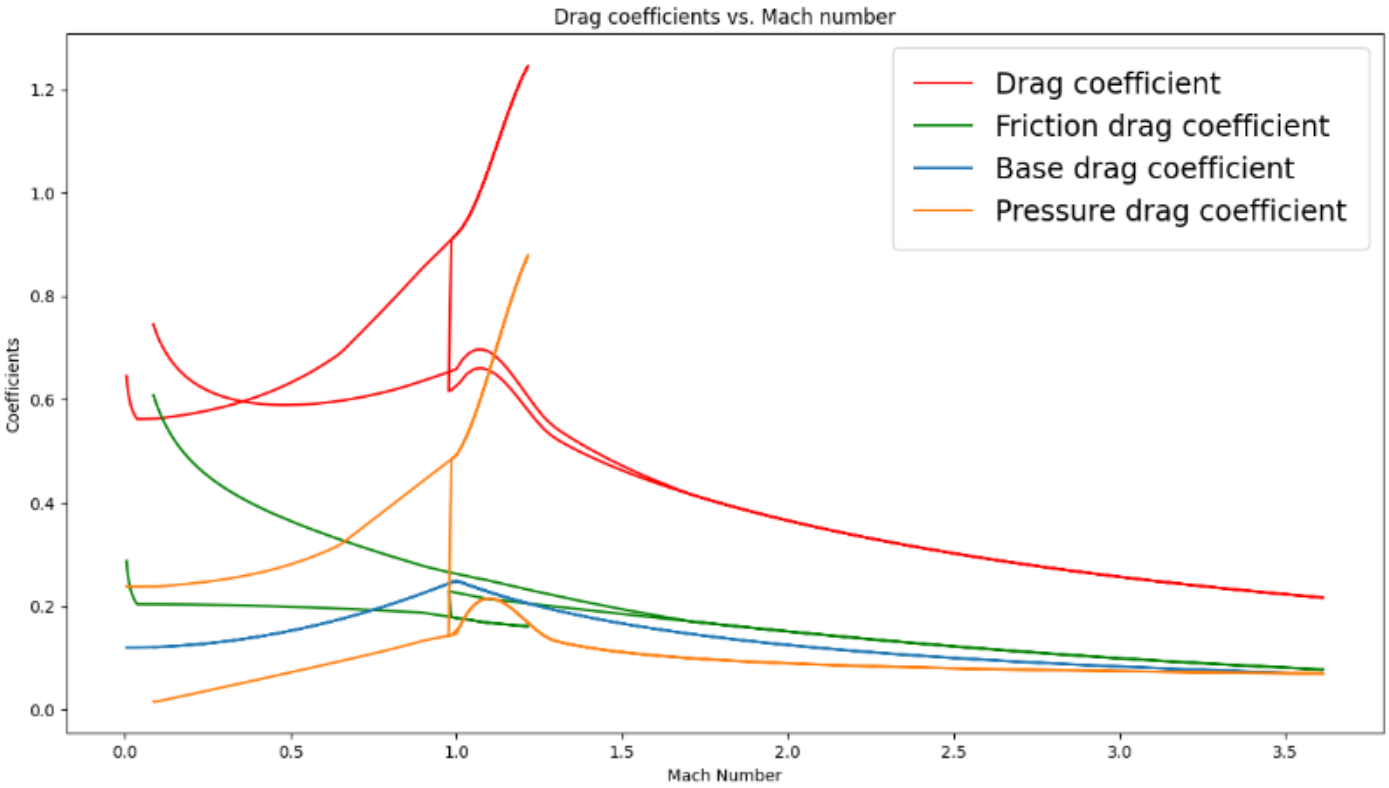

Fig. 11. Vehicle drag coefficients and a graph of the Mach number

Different forces due to pressure differences expose the launch vehicle to drags. Drag coefficient, base drag coefficient and pressure drag coefficient values show an increase up to 1 Mach level. The drag coefficient creates drag with a maximum value of 0.9. On the other hand, the friction drag coefficient value decreases. With the separation of the step, all drag coefficient values decreased. The largest drag type encountered at the 3.5 Mach level is the drag coefficient with a value of 0.25.

5. Conclusions

In this study, the launch vehicle that will carry the cubesat, which will be used for educational purposes, to the stratosphere layer has been full designed and flight analyzed. The design of the launch vehicle was carried out in accordance with the desired mission. The training cubesat was intended to be launched into the stratospheric layer in the earliest iterations of the launch vehicle. The cubesats will be dropped above the Kármán line in later iterations. Experiences were obtained by conducting a literature search.

In this study, the 10 kg payload was elevated to an altitude of 32676 m to create the launch vehicle design. The two stage launch vehicle has a total length of 419 cm and weighs 106602 g. The launch vehicle reaches supersonic speeds of Mach 3. Fiberglass, carbon fiber, aluminum and a composite materials were chosen to provide structural and thermal resistance at high speeds. A conical nose cone is designed to reduce the drag coefficient. Wedge type inactive ailerons are used to provide stable flight to the maximum altitude. Ailerons used in the second stage have a total drag coefficient of 0.02 and blades used in the first stage have a drag value of 0.05. Three reusable rocket engines were used in the first stage and one in the second stage. The launch vehicle has a maximum speed of 3.61 Mach, a maximum acceleration of 170 m/s^2, and an apogee of 32676 meters. The launch vehicle's pressure center is 321 cm from the reference plane, whereas the center of gravity is 269 cm from the same reference point.

Upon reaching an altitude of 3000 m, the initial stage of the launch vehicle separates, while the second stage ascends to approximately 32676 m, releasing the cubesat at its peak. The entire flight duration of the launch vehicle amounts to 725 seconds. Throughout the mission, stability is thoroughly examined and found to remain consistently positive. For the initial 10 seconds of flight, the center of gravity surpasses the center of pressure by an average of 100 cm. As the ascent continues for 80 seconds to the highest altitude, the center of gravity, on average, leads the center of pressure by 25 cm. The launch vehicle maintains a steady flight trajectory throughout its entire mission.

Different types of drag are discussed and analyzed. The drag coefficient, base drag coefficient, and pressure drag coefficient exhibit an increase up to the 1 Mach level. The drag coefficient reaches a maximum value of 0.9, generating the highest drag. Following the separation of the stage, all drag coefficient values decrease. At the 3.5 Mach level, the drag coefficient of 0.25 represents the largest encountered drag type.

In future studies, structural and flow analyzes will be examined in detail. A launch vehicle that can reach the Kármán Line, which is accepted as the space limit, and leave a cubesat, will be designed.

CRediT Author Statement

Alper Şanlı: Conceptualization, Methodology, Software, Investigation, Validation, Writing-Original Draft. **Tuncay Yunus Erkeç**: Conceptualization, Investigation, Resources. **Melih Beceren**: Conceptualization, Methodology, Software, Resources, Investigation, Validation, Writing-Original Draft. **Mehmet Furkan Kemallı**: Conceptualization, Methodology, Software, Investigation, Validation.

References

Balmogim, U., Brooks, M. J., Pitot de la Beaujardiere, J. F., Veale, K., Genevieve, B. and Roberts, L. W., 2015. Preliminary Design of the Phoenix-1B Hybrid Rocket. Orlando, 51st AIAA/SAE/ASEE Joint Propulsion Conference.

Barrowman, J.A., Theoretical Prediction of the Center of Pressure, Cambridge, 1966.

Bossert, D. E., Morris, S. L., Hallgren, W. F., & Yechout, T. R. (2003). Introduction to aircraft flight mechanics: Performance, static stability, dynamic stability, and classical feedback control. American Institute of Aeronautics and Astronautics.

Box, S., Bishop, C. Hunt, H., Estimating the dynamic and aerodynamic paramters of passively controlled high power rockets for flight simulaton, 2009.

Brooks, M. J., Pitot de la Beaujardiere, J. F., Chowdhury, S. M., Genevieve, B. and Roberts, L. W., 2010. Introduction to the Univeristy of KwaZulu-Natal Hybrid Sounding Rocket Program. Nashville, American Institude of Aeronautics and Astronautics.

Chowdhury, S. M., 2012. Design and Performance Simulation of a Hybrid Sounding Rocket,MScEng Thesis, Durban: University of KwaZulu-Natal.

Dyer, J., Doran, E., Dunn, Z., Lohner, K., Bayart, C., Sadhwani, A., Zilliac, G., Cantwel, B. and Karabeyoglu, A., 2007. Design and Development of a 100km Nitrous Oxide/Paraffin Hybrid Rocket Vehicle. Cincinnati, 43rd AIAA/ASME/SAE/ASEE

Joint Propulsion Conference and Exhibit.

Hall, H., Chamieh, M., Chu, J., Daruwala, R., Duong, V., Holt, S., ... & Stoica, A. (2020). Utilizing High Altitude Balloons as a Low-Cost CubeSat Test Platform. In 2020 IEEE Aerospace Conference (pp. 1-11). IEEE.

Johnstone, A. (2020). Cubesat Design Specification (1U-12U) Rev 14 CP-CDS-R14. The Cubesat Program, Cal Poly SLO, July.

Leverone, F. K., 2013. Performance Modelling and Simulation of a 100 km Hybrid Sounding Rocket, MScEng Thesis, Durban: University of KwaZulu-Natal.

Mahjub, A., Mazlan, N. M., Abdullah, M. Z., & Azam, Q. (2020). Design Optimization of Solid Rocket Propulsion: A Survey of Recent Advancements. Journal of Spacecraft and Rockets, 57(1), 3-11.

McCormick, A., Hultgren, E., Lichtman, M., Smith, J., Sneed, R. and Azimi, S., 2005. Design, Optimization, and Launch of a 3" Diameter N2O/Aluminized Paraffin Rocket. Tucson, 41st AIAA/ASME/SAE/ASEE Joint Propulsion Conference & Exhibit.

Mishra, A. K., Gandhi, K., Sharma, K., Sumanth, N., & Teja, Y. K. (2021). Conceptual design and analysis of two stage sounding rocket. International Journal of Universal Science and Engineering, 7(1), 52-72.

Sutton, G. P., & Biblarz, O. (2016). Rocket propulsion elements. John Wiley & Sons.

Şanlı, A., Aslan, A.R. (2021). Design of ASTINSAT-1 And Structural Analysis, Use of Generative Design. International Congress On Engineering And Technology Management.

Taylor, T. S. (2017). Introduction to rocket science and engineering. CRC Press.